Research Article | Vol. 28, No. 14 / 6 July 2020 / Optics Express 20449
Optics EXPRESS

# Topological charge of asymmetric optical vortices

VICTOR V. KOTLYAR AND ALEXEY A. KOVALEV*

*IPSI RAS – Branch of the FSRC "Crystallography and Photonics" RAS, 443001, Samara, Molodogvardeyskaya 151, Russia*
*alexeysmr@mail.ru

**Abstract:** We obtain theoretical relationships to define topological charge (TC) of vortex laser beams devoid of radial symmetry, namely asymmetric Laguerre-Gaussian (LG), asymmetric Bessel-Gaussian (BG), and asymmetric Kummer beams, as well as Hermite-Gaussian (HG) vortex beams. Although they are obtained as superposition of respective conventional LG, BG, and HG beams, these beams have the same TC equal to that of a single mode, $n$. At the same time, the normalized orbital angular momentum (OAM) that the beams carry is different, differently responding to the variation of the beam's asymmetry degree. However, whatever the asymmetry degree, TC of the beams remains unchanged and equals $n$. Although separate HG beam does not have OAM and TC, superposition of only two HG modes with adjacent numbers ($n$, $n+1$) and a $\pi/2$-phase shift produces a modal beam whose TC is -($2n+1$). Theoretical findings are validated via numerical simulation.



## 1. Introduction

Presently, laser vortex beams [1], or optical vortices (OV), have been actively studied because they have found uses in many optical applications. For instance, OVs are utilized in quantum information science [2], cryptography [3], wireless communication systems [4], data transmission in optical fibers [5], second-harmonic generation [6], short-pulse interferometry [7], and probing of turbulent media [8]. Vortex beams are characterized by two major parameters, namely, topological charge (TC) [9] and orbital angular momentum (OAM) [10], which describe different aspects of an OV. With TC depending only on the phase of a light field, OAM is both phase- and amplitude- (intensity) dependent. TC can be measured using a cylindrical lens [11] or a triangular aperture [12]. For measuring OAM, a cylindrical lens can also be utilized [13,14]. The OAM spectrum of OVs, which defines the energy contribution in each constituent angular harmonic of the laser beam, can be measured with a multi-order diffractive optical element [15] or based on intensity moments [16,17]. For radially symmetric OVs (e.g., LG and BG beams [18,19]), whose complex amplitude can be given by $E(r, \varphi, z) = A(r, z)\exp(in\varphi)$, where $A(r, z)$ is the radial component of the beam's complex amplitude, $n$ is TC of the beam, and ($r$, $\varphi$, $z$) are the cylindrical coordinates, TC is defined by OAM normalized to the beam's power and equals $n$. It is worth noting that an integer TC of a radially symmetric OV remains unchanged upon propagation. For other types of vortex beams, TC needs to be calculated individually. Meanwhile OAM of the beam remains unchanged upon propagation and can be calculated in the source plane, for TC this is not always the case. For instance, TC of a combined beam composed of two LG modes with different waist radii is not conserved [20].

In this work, we derive relationships to define TC of certain radially asymmetric vortex laser beams. In previous publications of the present authors, normalized OAMs of such beams were derived, but patterns of TC behavior were not analyzed. Below, we derive relationships to describe TC of asymmetric LG, BG, and Kummer beams [21,22,23], superposition of two HG modes [24], and a vortex HG beam [25]. We note that the considered asymmetrical beams are obtained by different ways. Asymmetric LG and Kummer beams are obtained from the

#394273 https://doi.org/10.1364/OE.394273
Journal © 2020 Received 3 Apr 2020; revised 20 May 2020; accepted 12 Jun 2020; published 25 Jun 2020

Optics EXPRESS

conventional symmetric LG and Kummer beams by a transverse complex shift in the Cartesian coordinates. Asymmetric BG beams are obtained by a hybrid technique: complex shift is applied only to the Bessel function, whereas the Gaussian function remains unshifted. Vortex HG beams are derived from the conventional HG beam by an astigmatic transform using a cylindrical lens. And another vortex beam is a superposition of two HG modes with complex weight coefficients. Therefore, we calculated TC for each type of the beam separately.

## 2. TC of an asymmetric LG beam

Upon free-space propagation of an asymmetric LG (aLG) beam, at a distance $z$ its complex amplitude is given by [21]

$$\begin{aligned} E(x,y,z) = {} & \frac{w(0)}{w(z)}\left[\frac{\sqrt{2}}{w(z)}\right]^{|l|}[(x-x_0)+i\theta(l)(y-y_0)]^{|l|}\times \\ & \times L_p^{|l|}\left[\frac{2\rho^2}{w^2(z)}\right]\exp\left[-\frac{\rho^2}{w^2(z)}+\frac{ik\rho^2}{2R(z)}-i(|l|+2p+1)\zeta(z)\right], \end{aligned} \tag{1}$$

where

$$\begin{aligned} \rho^2 &= (x-x_0)^2+(y-y_0)^2, \\ w(z) &= w\sqrt{1+\left(\frac{z}{z_R}\right)^2}, \\ R(z) &= z\left[1+\left(\frac{z_R}{z}\right)^2\right], \\ \zeta(z) &= \arctan\left(\frac{z}{z_R}\right), \end{aligned} \tag{2}$$

where $\theta(l) = \{1,\ l \geq 0;\ -1,\ l<0\}$, $(x,\ y,\ z)$ and $(r,\ \varphi,\ z)$ are the Cartesian and cylindrical coordinates, $(x_0,\ y_0)$ are the complex coordinates of the off-axis shift of the LG beam, $w$ is the Gaussian beam waist radius, $l$ is TC of the optical vortex, $L_p^l(x)$ is the associated Laguerre polynomial, $z_R = kw^2/2$ is the Rayleigh range, and $k = 2\pi/\lambda$ is the wavenumber of light of wavelength $\lambda$. The transverse intensity of the beam is not radially symmetric, unlike conventional LG beams [18]. If $(x_0,\ y_0)$ are real, beam (1) becomes a conventional off-axis LG mode.

Below, we discuss the TCs of various OVs derived in this work in relation with their OAMs derived in the previous studies. In doing so, we shall make use formulae for calculating OAM of paraxial laser beams and beam power [21]:

$$J_z = \mathrm{Im}\iint_{\mathbb{R}^2} E^*\left(x\frac{\partial E}{\partial y}-y\frac{\partial E}{\partial x}\right)dxdy, \tag{3}$$

$$W = \iint_{\mathbb{R}^2} E^*E dxdy. \tag{4}$$

For an aLG beam, OAM normalized to power is given by [21]

$$\frac{J_z}{W} = l + \frac{2\mathrm{Im}(x_0^*y_0)}{w^2}\left[\frac{L_p^1\left(\frac{Q^2}{2w^2}\right)}{L_p\left(\frac{Q^2}{2w^2}\right)}+\frac{L_{p+l}^1\left(\frac{Q^2}{2w^2}\right)}{L_{p+l}\left(\frac{Q^2}{2w^2}\right)}-1\right]. \tag{5}$$

where

$$Q = 2i\sqrt{(\mathrm{Im}x_0)^2+(\mathrm{Im}y_0)^2}. \tag{6}$$

Unlike TC, an increase or decrease in OAM is fully determined by the sign of the quantity $\mathrm{Im}(x_0^*y_0)$, because the relation in square brackets in Eq. (5) is always larger than or equal to unit.

Optics EXPRESS

Below, we calculate the TC of an aLG beam of Eq. (1), using the Berry's formula [9]:

$$TC = \lim_{r\to\infty} \frac{1}{2\pi} \int_0^{2\pi} d\varphi \frac{\partial}{\partial\varphi} \arg E(r,\varphi) = \frac{1}{2\pi} \lim_{r\to\infty} \mathrm{Im} \int_0^{2\pi} d\varphi \frac{\partial E(r,\varphi)/\partial\varphi}{E(r,\varphi)}. \tag{7}$$

We note that the standard definition of the TC is the number of $2\pi$ phase changes on a closed loop. Unfortunately, this definition is not constructive, and does not allow analytical calculation of the TC of optical vortices. It is a great merit of M.V. Berry that he proposed a more constructive TC definition (7), which we use in this paper. Both of these definitions lead to the same result.

Assuming $(l>0)$ that the complex shift in (2) is given by $x_0 = aw$, $y_0 = iaw$, the term $[(x-x_0)+i(y-y_0)]^l$ in (1) takes a simple form $r^l e^{il\varphi}$, with the variable $\rho^2$ in (2) taking the following form: $\rho^2 = (x-x_0)^2 + (y-y_0)^2 = r^2 - 2awre^{i\varphi}$, where $a$ is a dimensionless constant whose magnitude defines the asymmetry of the beam. With due regard for the above considerations, the derivative with respect to the angle $\varphi$ of the function in Eq. (1) takes the form:

$$\begin{aligned} &\tfrac{\partial E(r,\varphi,z)}{\partial\varphi} = ilE(r,\varphi,z) - \\ &- \left[-\tfrac{1}{w^2(z)} + \tfrac{ik}{2R(z)}\right](2iawre^{i\varphi})E(r,\varphi,z) - \\ &- \tfrac{4iawre^{i\varphi}}{w^2(z)} \tfrac{1}{L_p^{|l|}(\xi)} \tfrac{d}{d\xi} L_p^{|l|}(\xi) E(r,\varphi,z), \end{aligned} \tag{8}$$

where

$$\xi = \frac{2\rho^2}{w^2(z)}$$

Substituting (8) into (7) yields ($w = w(0)$):

$$\begin{aligned} TC &= \tfrac{1}{2\pi} \lim_{r\to\infty} \mathrm{Im} \int_0^{2\pi} d\varphi \left\{ il - \left[-\tfrac{1}{w^2(z)} + \tfrac{ik}{2R(z)}\right](2iarwe^{i\varphi}) - \tfrac{i4awre^{i\varphi}}{w^2(z)} \tfrac{1}{L_m^{|l|}(\xi)} \tfrac{\partial L_m^{|l|}(\xi)}{\partial\xi} \right\} = \\ &= l + \lim_{r\to\infty} \mathrm{Re} \left[ \left(-\tfrac{2}{w^2(z)} + \tfrac{ik}{R(z)}\right) raw \int_0^{2\pi} d\varphi e^{i\varphi} \right] - \lim_{r\to\infty} \mathrm{Re} \int_0^{2\pi} d\varphi \tfrac{2r|l|awe^{i\varphi}}{r(r-2awe^{i\varphi})} = l. \end{aligned} \tag{9}$$

In deriving the third term in (9), in the limiting case of $r\to\infty$, we utilized the asymptotic formula for the associated Laguerre polynomials: $[L_p^{|l|}(x)]^{-1}\partial L_p^{|l|}(x)/\partial x \approx |l|/x$. Thus, at $r\to\infty$, the third term in (9) equals zero, because the radial variable $r$ has the first degree in the numerator and second degree in the denominator. The second term in (9) is also zero but for a different reason. Here, notwithstanding the presence of the radial variable $r$, which tends to infinity, there is also an integral function $\exp(i\varphi)$ integrated from 0 to $2\pi$, which equals zero. From Eq. (9), TC of an aLG mode is seen to equal $l$. Thus, for a conventional LG mode, a complex shift of coordinates causes changes in its form [Eq. (1)] and OAM [Eq. (5)], with its TC [Eq. (9)] remaining unchanged. We also note that for the aLG beam of Eq. (1), TC remains equal to $l$ upon propagation because Eq. (9) is valid for any $z$.

In this section, we denoted the topological charge as $l$, which is commonly used for LG beams. In the next sections, we denote TC as $n$.

## 3. TC of an asymmetric BG beam

The complex amplitude of a BG beam [19] in the source plane $z=0$ can be given by

$$E_n(r,\varphi,z=0) = \exp\left(-\frac{r^2}{\omega_0^2} + in\varphi\right) J_n(\alpha r), \tag{10}$$

where $\alpha = k\sin\theta_0 = (2\pi/\lambda)\sin\theta_0$ is a scaling factor, $k = 2\pi/\lambda$ is the wavenumber of light of wavelength $\lambda$, $\theta_0$ is the angle of a conical wave that forms a Bessel beam. In any other plane $z$,

Optics EXPRESS

the complex amplitude (10) takes the form:

$$E_n(r,\varphi,z) = q^{-1}(z)\exp\left(ikz - \frac{i\alpha^2 z}{2kq(z)}\right)\exp\left(-\frac{r^2}{\omega_0^2 q(z)} + in\varphi\right)J_n\left[\frac{\alpha r}{q(z)}\right], \tag{11}$$

where $q(z) = 1 + iz/z_0$, $z_0 = k\omega_0^2/2$ is the Rayleigh range, $\omega_0$ is the radius waist of the Gaussian beam, $J_n(x)$ is the Bessel function of the first kind and $n$-th order. For an asymmetric Bessel-Gaussian (aBG) beam, the complex amplitude takes the form [22]:

$$\begin{aligned} E_n(r,\varphi,z;c) &= \tfrac{1}{q(z)}\exp\left(ikz - \tfrac{i\alpha^2 z}{2kq(z)} - \tfrac{r^2}{q(z)\omega_0^2} + in\varphi\right)\times \\ &\times\left[\tfrac{\alpha r}{\alpha r - 2cq(z)\exp(i\varphi)}\right]^{n/2} J_n\left\{\tfrac{1}{q(z)}\sqrt{\alpha r[\alpha r - 2cq(z)\exp(i\varphi)]}\right\}. \end{aligned} \tag{12}$$

In Eq. (12), $c$ is a dimensionless constant that defines the asymmetry of the aBG beam. Unlike the aLG beam of Eq. (1), the aBG beam of Eq. (12) is derived not through a complex shift of coordinates but through superposition of conventional Bessel beams, which is mathematically expressed using a reference series [22]:

$$\sum_{k=0}^{\infty}\frac{t^k}{k!}J_{k+\nu}(x) = x^{\nu/2}(x-2t)^{-\nu/2}J_\nu\left(\sqrt{x^2-2tx}\right). \tag{13}$$

It is possible to derive a relationship for OAM carried by the aBG beam, normalized to power [22]:

$$\frac{J_z}{W} = n + \left[\sum_{p=0}^{\infty}\frac{c^{2p}pI_{n+p}(y)}{(p!)^2}\right]\cdot\left[\sum_{p=0}^{\infty}\frac{c^{2p}I_{n+p}(y)}{(p!)^2}\right]^{-1}, \tag{14}$$

where $y = \alpha^2\omega_0^2/4$. We did not manage to further simplify Eq. (14). From Eq. (14), OAM of the aBG beams is seen to be larger than $n$, because all constituent terms of the series in (14) are positive. Thus, with increasing parameter $c$, asymmetry of the aBG beam increases and OAM also increases near linearly. Growth of the OAM (14) follows partly from the series (13), where all Bessel functions have the order higher than that of the Bessel function in the aBG beam from Eq. (12). Physical reason of the OAM growth with the asymmetry degree is that the 'center of mass' [26] of the aBG beam shifts from the singularity center located in the origin [22]. TC of the aBG beam in Eq. (12) can be found using Eq. (7). First, write down the derivative of function (12) with respect to the azimuthal angle (assuming $J_n(x) \neq 0$, to avoid dividing by zero):

$$\begin{aligned} \tfrac{\partial E_n(r,\varphi,z;c)}{\partial\varphi} &= inE_n(r,\varphi,z;c) + \\ &+\tfrac{incq(z)e^{i\varphi}}{(\alpha r - 2cq(z)\exp(i\varphi))}E_n(r,\varphi,z;c) - \\ &-\tfrac{ic(\alpha r)^{1/2}e^{i\varphi}J_n^{-1}(x)}{(\alpha r - 2cq(z)\exp(i\varphi))^{1/2}}\tfrac{\partial J_n(x)}{\partial x}E_n(r,\varphi,z;c), \end{aligned} \tag{15}$$

where $x = q^{-1}(z)\{\alpha r[\alpha r - 2cq(z)\exp(i\varphi)]\}^{1/2}$. Then, Eq. (7) takes the form:

$$\begin{aligned} TC &= \tfrac{1}{2\pi}\lim_{r\to\infty}\mathrm{Re}\int_0^{2\pi}d\varphi\left\{n + \tfrac{ncq(z)e^{i\varphi}}{[\alpha r - 2cq(z)e^{i\varphi}]} - \tfrac{c(\alpha r)^{1/2}e^{i\varphi}}{[\alpha r - 2cq(z)e^{i\varphi}]^{1/2}}\tfrac{1}{J_n(x)}\tfrac{\partial J_n(x)}{\partial x}\right\} = \\ &= n + \lim_{r\to\infty}\mathrm{Re}\left[\tfrac{cJ_n^{-1}(x)}{2\pi}\tfrac{\partial J_n(x)}{\partial x}\int_0^{2\pi}d\varphi e^{i\varphi}\right] = n. \end{aligned} \tag{16}$$

In Eq. (16), the second term of the integrand tends to zero at $r \to \infty$, because in the denominator the radial variable $r$ is has the first degree. Although for a different reason, the third term is also

Optics EXPRESS

rearranged to a zero-valued term because it contains a ratio of the derivative of a Bessel function to a Bessel function. At $r \to \infty$, the said ratio can take any value since at a large argument, the asymptotic functions of a Bessel function and the derivative thereof are given by

$$\begin{aligned} J_n(x>>1) &\approx \sqrt{\tfrac{2}{\pi x}}\cos\left(x - \tfrac{n\pi}{2} - \tfrac{\pi}{4}\right), \\ \tfrac{dJ_n}{dx}(x>>1) &\approx -\sqrt{\tfrac{2}{\pi x}}\sin\left(x - \tfrac{n\pi}{2} - \tfrac{\pi}{4}\right), \end{aligned} \tag{17}$$

with their ratio given by a tangent. The third term of Eq. (16) also contains an integral of $\exp(i\varphi)$ taken with respect to the angle $\varphi$ from 0 to $2\pi$, which equals zero, making the entire term equal zero. From Eq. (16) it follows that at any asymmetry degree (any $c$) and any distance from the source plane (any $z$) of an aBG beam, TC equals $n$. Meanwhile OAM of the aBG beam increases with increasing asymmetry degree, Eq. (14).

## 4. TC of an asymmetric Kummer beam

Asymmetric Kummer beams (aK beams) that represent exact solutions of a paraxial Helmholtz equation have been reported [23]. The complex amplitude of an aK beam is deduced by shifting a conventional hypergeometric or Kummer beam [23] into a complex coordinate plane ($x \to x - aw$, $y \to y - iaw$, where $a$ is a dimensionless real number) at any $z$:

$$\begin{aligned} E_s(r,\varphi,z) = \tfrac{(-i)^{n+1}}{n!}\Gamma\left(\tfrac{m+n+2+i\gamma}{2}\right)\left(\tfrac{z_0}{zq(z)}\right)q^{-(m+i\gamma)/2}(z)\times \\ \times\left(\tfrac{kwr}{2z\sqrt{q(z)}}\right)^n \exp\left(in\varphi + \tfrac{iks^2}{2z}\right){}_1F_1\left(\tfrac{m+n+2+i\gamma}{2}, n+1, -\xi\right), \end{aligned} \tag{18}$$

where $s^2 = r(r - 2awe^{i\varphi})$, $\xi = [kws/(2zq^{1/2}(z))]^2$ and ${}_1F_1(a,b,z)$ is a Kummer function (degenerate hypergeometric function). In the source plane ($z = 0$), the complex amplitude Eq. (18) of a shifted Kummer beam takes the form:

$$E_s(r,\varphi,z=0) = \frac{r^n e^{in\varphi}}{w^n}\left(\frac{s}{w}\right)^{m-n+i\gamma}\exp\left(-\frac{s^2}{w^2}\right), \tag{19}$$

The derivative of Eq. (19) with respect to $\varphi$ is

$$\frac{\partial E}{\partial \varphi} = inE - (m - n + i\gamma)\frac{irawe^{i\varphi}}{s^2}E + \frac{2irae^{i\varphi}}{w}E. \tag{20}$$

Substituting Eq. (20) in Eq. (7) yields:

$$\begin{aligned} TC = \tfrac{1}{2\pi}\lim_{r\to\infty}\mathrm{Im}\int_0^{2\pi} d\varphi\left(in - \tfrac{i(m-n+i\gamma)rawe^{i\varphi}}{r(r-2awe^{i\varphi})} + \tfrac{2irae^{i\varphi}}{w}\right) = \\ = n + \tfrac{ar}{\pi w}\int_0^{2\pi}\cos\varphi d\varphi = n. \end{aligned} \tag{21}$$

The integrand in Eq. (21) contains three terms, with the first equal to $n$ and second equal to zero at $r \to \infty$ (considering that the radial variable $r$ has power two in the denominator and power one in numerator). The third term also equals zero because the integral of cosine function taken with respect to the angle on a period exactly equals zero, despite being multiplied by infinity at $r \to \infty$. Thus, in the source plane, an aK beam has TC equal to $n$. Using Eq. (18), it can be shown in a similar way that at any $z$ TC Eq. (18) equals $n$.

Optics EXPRESS

## 5. TC of an OV composed of two HG modes

It has previously been demonstrated [24] that superposition of two HG modes, $(n,\ n+1)$ and $(n+1,\ n)$, with a phase shift by $\pi/2$ generates an OV that carries OAM proportional to -$(n+1)$. In this section, we obtain a relationship to define TC of such an OV. In the source plane ($z=0$), superposition of two HG beams has the complex amplitude given by

$$\begin{aligned} E(x,y,0) &= \exp\left[-\tfrac{w^2}{2}(x^2+y^2)\right]\times \\ &\times[H_n(wx)H_{n+1}(wy) + i\gamma H_{n+1}(wx)H_n(wy)] \end{aligned}, \tag{22}$$

where $w=\sqrt{2}/w_0$, $w_0$ is the Gaussian beam waist radius, also assuming constant $\gamma=1$. For light field Eq. (22), the normalized OAM for any integer $n$ can be written as [24]:

$$\frac{J_z}{W} = -(n+1). \tag{23}$$

Owing to the fact that the sum of the numbers in both modes in Eq. (22) is the same, the linear combination thereof in Eq. (22) is also a mode, with both constituent modes having the same Gouy phase ($(m+n+1)\arctan(z/z_0)$), which retains its form upon propagation, changing only in scale.

Even before one starts calculating TC from Eq. (7), the answer can be predicted in advance. Actually, the first term in Eq. (22) has $n$ vertical zero lines and $(n+1)$ horizontal zero lines. Meanwhile the second term in Eq. (22), on the contrary, has $(n+1)$ vertical zero lines (which do not coincide with those of the first term) and $n$ horizontal zero lines. Hence, the intensity nulls in Eq. (22) are found at intersection points of the horizontal and vertical zero lines. There are $n^2$ intersection points in the vicinity of zero $x+iy$ and $(n+1)^2$ intersection points in the vicinity of zero $y+ix$. Therefore, for field Eq. (22), TC is defined by $TC = n^2-(n+1)^2 = -(2n+1)$.

To determine TC of the beam by its complex amplitude Eq. (22), we express HG modes in Eq. (22) via LG modes (expression (3.11) in [27]):

$$\begin{aligned} i^m H_n(\xi)H_m(\eta) = {\sum_{k=0}^{[(n+m)/2]}}' (-2)^k k! P_k^{(n-k,m-k)}(0)\times \\ \times[(\xi+i\eta)^{n+m-2k} + (-1)^m(\xi-i\eta)^{n+m-2k}]L_k^{n+m-2k}(\xi^2+\eta^2), \end{aligned} \tag{24}$$

where $P$ are the Jacobi polynomials and the hatch near the sum means that for even numbers $n$ and $m$ the last term should be divided by 2. Then, products of the Hermite polynomials in Eq. (22) read as

$$\begin{aligned} H_n(wx)H_{n+1}(wy) = i^{-n-1}\sum_{k=0}^{n}(-2)^k k! P_k^{(n-k,n+1-k)}(0) w^{2n+1-2k} \\ \times L_k^{2n+1-2k}(w^2x^2+w^2y^2)[(x+iy)^{2n+1-2k} + (-1)^{n+1}(x-iy)^{2n+1-2k}], \end{aligned} \tag{25}$$

$$\begin{aligned} H_{n+1}(wx)H_n(wy) = i^{-n}\sum_{k=0}^{n}(-2)^k k! P_k^{(n+1-k,n-k)}(0) w^{2n+1-2k} \\ \times L_k^{2n+1-2k}(w^2x^2+w^2y^2)[(x+iy)^{2n+1-2k} + (-1)^{n}(x-iy)^{2n+1-2k}]. \end{aligned} \tag{26}$$

Using these expressions, we can rewrite Eq. (22) in the polar coordinates:

$$\begin{aligned} E(r,\varphi,0) = (-i)^{n+1}\exp\left(-\tfrac{w^2r^2}{2}\right)\sum_{k=0}^{n}(-2)^k k!(wr)^{2n+1-2k}L_k^{2n+1-2k}(w^2r^2) \\ \times[A_k^- e^{i(2n+1-2k)\varphi} - (-1)^n A_k^+ e^{-i(2n+1-2k)\varphi}]. \end{aligned} \tag{27}$$

where $A_k^{\pm}=P_k^{(n-k,n+1-k)}(0) \pm P_k^{(n+1-k,n-k)}(0)$.

Optics EXPRESS

Thus, we obtained a superposition of a finite number of LG modes. Such finite superposition has the TC equal to that of the LG mode with the highest (by modulus) order [28]. There are two such modes in Eq. (27) (at $k = 0$), and therefore TC of such superposition equals either $2n + 1$ or $-(2n + 1)$, depending on which mode has the greater weight coefficient. It is known for the Jacobi polynomials that [29]

$$P_k^{(\alpha,\beta)}(-z) = (-1)^k P_k^{(\beta,\alpha)}(z). \tag{28}$$

Therefore, $P_0^{(n,n+1)}(0) = P_0^{(n+1,n)}(0)$ and the weight coefficient $A_0^-$ of the LG mode of the order $2n + 1$ equals zero. Thus, TC of the superposition of two HG beams Eq. (22) is given by

$$TC = -(2n + 1). \tag{29}$$

To get the positive topological charge $TC = 2n + 1$, one can swap the variables $x$ and $y$ in Eq. (22).

## 6. TC of a vortex HG beam

It has been shown [25] that it is possible to superimpose several HG modes using a reference expression from [29]

$$\sum_{k=0}^{n} \frac{n!\, t^k}{k!(n-k)!} H_k(x) H_{n-k}(y) = (1 + t^2)^{n/2} H_n\left(\frac{tx + y}{\sqrt{1 + t^2}}\right), \tag{30}$$

it is possible to generate a vortex HG beam whose complex amplitude is given by

$$U_n(x, y, z) = i^n \exp\left(-\frac{x^2 + y^2}{2}\right)(1 - a^2)^{n/2} H_n\left(\frac{iax + y}{\sqrt{1 - a^2}}\right). \tag{31}$$

Considering that in superposition Eq. (30) the sum of numbers of the constituent HG modes is constant, $k + (n - k) = n = \text{const}$, all constituent HG modes in Eq. (30) have the same phase velocity (i.e. the same Gouy phases, $(n + m + 1)\arctan(z/z_0)$), meaning that the whole beam Eq. (31) is a paraxial mode, which retains its transverse intensity structure upon propagation, only changing in scale and rotating. OAM of beam Eq. (31) is given by [25]

$$\frac{J_z}{W} = -\frac{2an}{1 + a^2}. \tag{32}$$

The real parameter $a$ in Eq. (31) and Eq. (32) can be related to the rotation angle $\alpha$ of a cylindrical lens [11,27] that converts a conventional HG beam $(0, n)$ into a vortex HG beam in Eq. (31):

$$\cos\alpha = \frac{a}{\sqrt{1 + a^2}}, \quad \sin\alpha = \frac{1}{\sqrt{1 + a^2}}. \tag{33}$$

Let us derive TC of vortex HG beam Eq. (31) substituting Eq. (31) into Eq. (7), which gives:

$$\begin{aligned} TC &= \tfrac{1}{2\pi} \lim_{r\to\infty} \mathrm{Im} \int_0^{2\pi} d\varphi \tfrac{\partial E(r,\varphi)/\partial\varphi}{E(r,\varphi)} = \\ &= \tfrac{n}{2\pi} \lim_{r\to\infty} \mathrm{Im} \int_0^{2\pi} d\varphi \tfrac{H_{n-1}(ir\cos\varphi\cos\alpha + r\sin\varphi\sin\alpha)(-ir\sin\varphi\cos\alpha + r\cos\varphi\sin\alpha)}{H_n(ir\cos\varphi\cos\alpha + r\sin\varphi\sin\alpha)}. \end{aligned} \tag{34}$$

Putting $r \to \infty$ in Eq. (34) and replacing the Hermite polynomials with the highest-power monomials, $H_n(x>>1) \approx (2x)^n$, Eq. (34) is rearranged to

$$\begin{aligned} TC &= \tfrac{1}{2\pi} \mathrm{Im} \int_0^{2\pi} d\varphi \tfrac{n(-i\sin\varphi\cos\alpha + \cos\varphi\sin\alpha)}{(i\cos\varphi\cos\alpha + \sin\varphi\sin\alpha)} = \\ &= \tfrac{-n}{2\pi} \int_0^{2\pi} d\varphi \tfrac{\tan\alpha}{\cos^2\varphi + \tan^2\alpha\sin^2\varphi} = -n. \end{aligned} \tag{35}$$

Optics EXPRESS

In deriving Eq. (35), the reference integral was used [29]:

$$\int_0^{2\pi} \frac{d\varphi}{\cos^2\varphi + \gamma^2 \sin^2\varphi} = \frac{2\pi}{\gamma}. \tag{36}$$

From comparison of relationships for OAM in Eq. (32) and TC in Eq. (35) of the vortex HG beam, TC is seen to depend neither on the parameter $a$ nor the tilt angle $\alpha$ of the cylindrical lens [Eq. (33)], with OAM being dependent of the parameter $\alpha$. We note that to make the topological charge Eq. (35) of the vortex HG beam positive, one can swap the variables $x$ and $y$.

Because of this, both OAM and TC are equally important characteristics when describing OVs.

## 7. Numerical simulation

Figure 1 depicts intensity and phase patterns for an aBG beam of Eq. (12) in three transverse planes: $z = 0$ [source plane, Figs. 1(a) and 1(b)], $z = z_0$ [at the Rayleigh range, Figs. 1(c) and 1(d)], and $z = 10z_0$ [far field, Figs. 1(e) and 1(f)]. In the source plane, alongside an OV of eight-order a multitude of OVs of the first order can be observed. At the Rayleigh range, the only vortex can be found in the left bottom of Fig. 1(d). In the far field, the only remaining vortex is the central

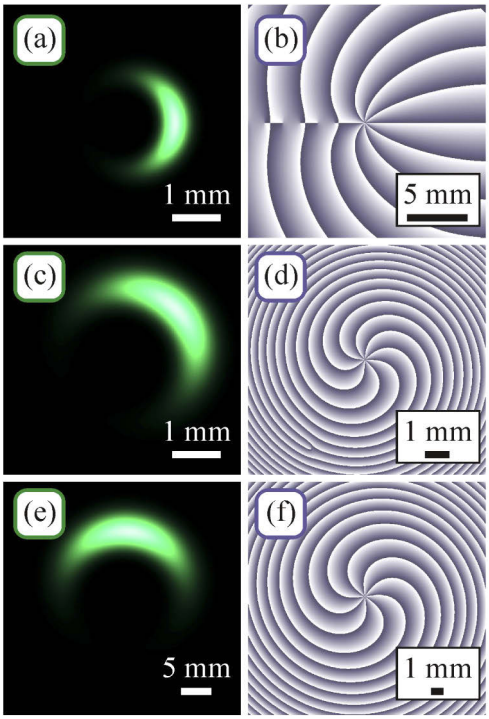


**Fig. 1.** Patterns of intensity (a, c, e) and phase (b, d, f) for an aBG beam in three different planes. Simulation was conducted at a wavelength of $\lambda = 532$ nm, beam radius $w_0 = 0.5$ mm, an OV of the eighth order $n = 8$, scaling factor $\alpha = 1/w_0$, asymmetry parameter $c = w_0/40$, propagation distance $z = 0$ (source plane) (a,b), $z = z_0$ (Rayleigh range) (c,d), and $z = 10z_0$ (far field) (e,f), for the calculation domain $-R \le x, y \le R$, where $R = 10$ mm ($z = 0$), $R = 10$ mm ($z = z_0$), and $R = 20$ mm ($z = 10z_0$), and the number of pixels $2048 \times 2048$. TC was calculated along a circle of $x^2 + y^2 = {R_1}^2$, where $R_1 = 0.8R$. The resulting values of TC are 11.9926 (a,b), 8.8837 (c,d), and 7.9393 (e,f).

Optics EXPRESS

OV of the eighth order. The numerical simulation gave the following values of TC: 11.9926 (at $z = 0$), 8.8837 (at $z = z_0$), and 7.9393 (at $z = 10z_0$).

Figure 2 depicts similar patterns of intensity and phase distributions of aLG beam (1) in three transverse planes: $z = 0$ [source plane, Figs. 2(a) and 2(b)], $z = z_0$ [at the Rayleigh range, Figs. 2(c) and 2(d)], and $z = 10z_0$ [far field, Figs. 2(e) and 2(f)]. In the source plane, alongside an eighth-order OV there are several first-order OVs. At the Rayleigh range, there are several such vortices, with three OVs clearly seen on the left of the center in Fig. 1(d). In the far field, only an eighth-order central OV is seen. The numerically simulated values of TC are 7.9974 (at $z = 0$), 7.9925 (at $z = z_0$), and 7.9226 (at $z = 10z_0$).

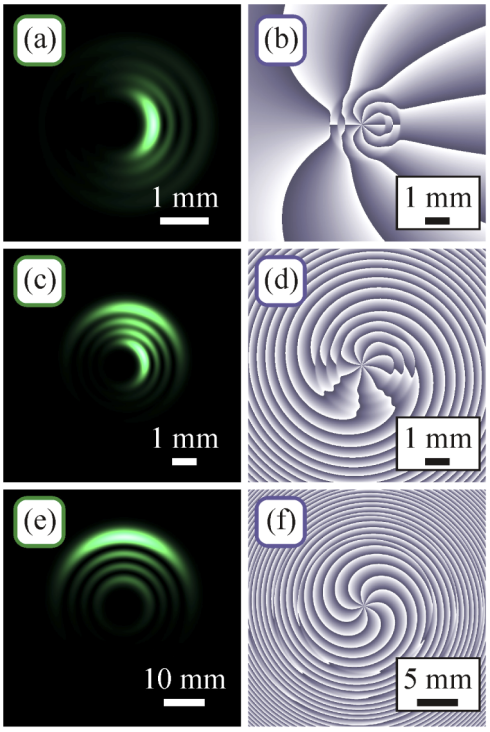


**Fig. 2.** Patterns of intensity (a,c,e) and phase (b,d,f) for an aLG beam in three different planes. The simulation was conducted at a wavelength of $\lambda = 532$ nm, waist radius $w_0 = 0.5$ mm, OV order $n = 8$, mode radial index $m = 3$, shift vector $(x_0, y_0) = (0, iw_0/4)$, propagation distance $z = 0$ (source plane) (a,b), $z = z_0$ (Rayleigh range) (c,d), and $z = 10z_0$ (far field) (e,f), computation domain $-R \le x, y \le R$, where $R = 5$ mm ($z = 0$), $R = 5$ mm ($z = z_0$), $R = 30$ mm ($z = 10z_0$), and the number of pixels 2048 × 2048. TC was calculated along a circle of radius $x^2 + y^2 = {R_1}^2$, where $R_1 = 0.8R$. The resulting values of TC are 7.9974 (a,b), 7.9925 (c,d), and 7.9226 (e,f).

Figure 3 depicts patterns of intensity and phase of an asymmetric Kummer function in Eq. (18) in three transverse planes: $z = 0$ [source plane, Figs. 3(a) and 3(b)], $z = z_0$ [Rayleigh length, Figs. 3(c) and 3(d)], and $z = 10z_0$ [far field, Figs. 3(e) and 3(f)]. It is seen that despite the asymmetric intensity pattern, in all the planes of interest there is a first-order OV at the center. The numerically calculated values of TC are 0.9981 (at $z = 0$), 0.9992 (at $z = z_0$), and 0.9999 (at $z = 10z_0$).

Figure 4 depicts patterns of intensity and phase for superposition of two HG modes Eq. (22) in the source plane. Despite a great number of isolated intensity nulls, almost all of them are seen to compensate each other (OVs of the plus and minus first order), with only a limited number

Optics EXPRESS

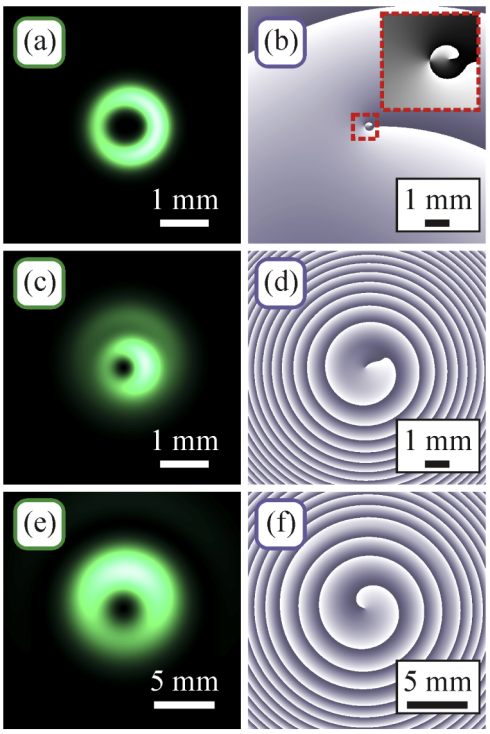


**Fig. 3.** Patterns of intensity (a,c,e) and phase (b,d,f) for an asymmetric Kummer beam in three different planes. The simulation was conducted at a wavelength of $\lambda = 532$ nm, waist radius of the Gaussian beam, $w_0 = 0.5$ mm, OV order $n = 1$, parameters $m$ and $\gamma$ taken to be $m = 3$ and $\gamma = 0$, shift parameter $a = 0.2$, propagation distance $z = 0$ (source plane) (a,b), $z = z_0$ (Rayleigh length) (c,d), and $z = 10z_0$ (far field) (e,f), computation domain $-R \le x$, $y \le R$, where $R = 5$ mm ($z = 0$), $R = 5$ mm ($z = z_0$), $R = 10$ mm ($z = 10z_0$), in each plot, the number of pixels is 2048 × 2048. The inset in Fig. 3(b) depicts a magnified central fragment. TC was calculated along a circle of radius $x^2 + y^2 = {R_1}^2$, where $R_1 = 0.8$R. The resulting values of TC are 0.9981 (a,b), 0.9992 (c,d), and 0.9999 (e,f).

of phase jumps remaining at infinity. The numerically simulated value of TC equals –10.9550, corresponding to a theoretically predicted value of $-(2n + 1)$ at $n = 5$.

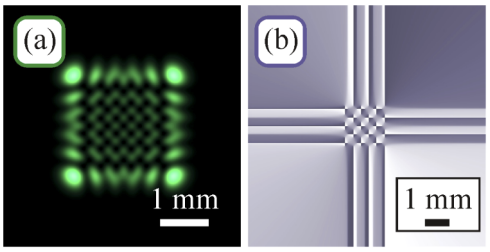


**Fig. 4.** Patterns of intensity (a) and phase (b) for the sum of two HG modes in the source plane. The simulation was conducted at a wavelength of $\lambda = 532$ nm, waist radius of the Gaussian beam $w_0 = 0.5$ mm, OV order $n = 5$, computation domain $-R \le x$, $y \le R$, where $R = 5$ mm, the number of pixels 2048 × 2048. TC was calculated along a circle of radius $x^2 + y^2 = {R_1}^2$, where $R_1 = 0.8R$. The resulting TC is -10.9550.

Optics EXPRESS

Figure 5 depicts patterns of intensity and phase for the vortex HG modes Eq. (31) in the source plane. On the vertical axis, there are ten isolated intensity nulls of the minus first order, the sum of which give TC equal to –10. The numerically simulated value of TC is –9.9993.

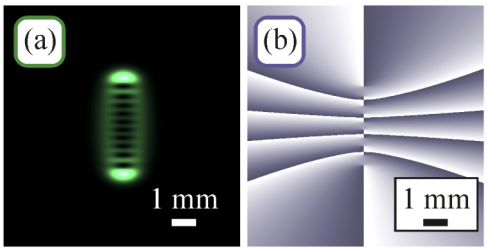


**Fig. 5.** Patterns of intensity (a) and phase (b) for a vortex HG mode in the source plane. The simulation was conducted at a wavelength of $\lambda = 532$ nm, waist radius of the Gaussian beam $w_0 = 0.5$ mm, OV order $n = 10$, asymmetry parameter $a = 0.3$, computation domain $-R \le x$, $y \le R$, where $R = 5$ mm, and the number of pixels is 2048 × 2048. TC was numerically calculated along a circle $x^2 + y^2 = {R_1}^2$, where $R_1 = 0.8R$. The resulting TC value is -9.9993.

## 8. Conclusion

In this work, we have shown that if familiar radially symmetric laser beams (like LG and Kummer beams) are modified by shifting the coordinate system in a complex plane, both the form of the transverse intensity pattern and OAM are also changed depending on the degree of asymmetry, whereas TC of the asymmetric LG and Kummer beams remains unchanged and equals $n$. It has also been shown that if a familiar radially symmetric BG beam with TC = $n$ undergoes a hybrid transformation in which the Gaussian beam remains unchanged while the Bessel beam is shifted into the complex plane, in the resulting asymmetric BG beam TC remains unchanged TC = $n$. The HG beam has been known to carry no TC, being topologically neutral. After passing through a cylindrical lens whose axis makes a certain angle with the Cartesian axes, the resulting vortex HG beam will carry OAM depending on the rotation angle of the cylindrical lens. However, TC of such a beam has been found to be independent of the cylindrical lens rotation, being equal to $n$. A vortex HG beam is finite superposition of conventional vortex-free HG beams. We have shown that a vortex beam can be generated by superimposing just two conventional HG beams with the numbers ($n$, $n + 1$) and ($n + 1$, $n$) and a π/2-phase shift. In the resulting vortex HG beam, TC equals $-(2n + 1)$.

## Funding

Russian Foundation for Basic Research (18-29-20003); Russian Science Foundation (18-19-00595); Ministry of Science and Higher Education of the Russian Federation.

## Acknowledgments

This work was partly funded by the Russian Foundation of Basic Research under grant # 18-29-20003 (calculation of TC of asymmetric OVs), Russian Science Foundation under grant # 18-19-00595 (calculation of TC of vortex HG beams), and RF Ministry of Science and Higher Education under the government project of FSRC for “Crystallography and Photonics” RAS (numerical simulation).

## Disclosures

The authors declare that there are no conflicts of interest related to this article.

Optics EXPRESS

## References


1. V. V. Kotlyar, A. A. Kovalev, and A. P. Porfirev, Vortex laser beams (CRC Press: Boca Raton, 2019).
2. S. Li, X. Pan, Y. Ren, H. Liu, S. Yu, and J. Jing, "Deterministic generation of orbital-angular-momentum multiplexed tripartite entanglement," Phys. Rev. Lett. **124**(8), 083605 (2020).
3. M. Hiekkamaki, S. Prabhakar, and R. Fickler, "Near-perfect measuring of full-field transverse-spatial modes of light," Opt. Express **27**(22), 31456–31464 (2019).
4. S. Li, X. Li, L. Zhang, G. Wang, L. Zhang, M. Liu, C. Zeng, L. Wang, Q. Sun, W. Zhao, and W. Zhang, "Efficient optical angular momentum manipulation for compact multiplexing and demultiplexing using a dielectric metasurface," Adv. Opt. Mater. **8**(8), 1901666 (2020).
5. A. Pryamikov, G. Alagashev, G. Falkovich, and S. Turitsyn, "Light transport and vortex-supported wave-guiding in micro-strustured optical fibers," Sci. Rep. **10**(1), 2507 (2020).
6. K. Dai, W. Li, K. S. Morgan, Y. Li, J. K. Miller, R. J. Watkins, and E. G. Johnson, "Second-harmonic generation of asymmetric Bessel-Gaussian beams carrying orbital angular momentum," Opt. Express **28**(2), 2536–2546 (2020).
7. N. Dimitrov, M. Zhekova, G. G. Paulus, and A. Dreischuh, "Inverted field interferometer for measuring the topological charges of optical vortices carried by short pulses," Opt. Commun. **456**, 124530 (2020).
8. R. J. Watkins, K. Dai, G. White, W. Li, J. K. Miller, K. S. Morgan, and E. G. Johnson, "Experimental probing of turbulence using a continuous spectrum of asymmetric OAM beams," Opt. Express **28**(2), 924–935 (2020).
9. M. V. Berry, "Optical vortices evolving from helicoidal integer and fractional phase steps," J. Opt. A: Pure Appl. Opt. **6**(2), 259–268 (2004).
10. L. Allen, M. Beijersbergen, R. Spreeuw, and J. Woerdman, "Orbital angular momentum of light and the transformation of Laguerre-Gaussian laser modes," Phys. Rev. A **45**(11), 8185–8189 (1992).
11. V. V. Kotlyar, A. A. Kovalev, and A. P. Pofirev, "Astigmatic transforms of an optical vortex for measurement of its topological charge," Appl. Opt. **56**(14), 4095–4104 (2017).
12. J. M. Hickmann, E. J. S. Fonseca, W. C. Soares, and S. Chavez-Cerda, "Unveiling a truncated optical lattice associated with a triangular aperture using lights orbital angular momentum," Phys. Rev. Lett. **105**(5), 053904 (2010).
13. S. N. Alperin, R. D. Niederriter, J. T. Gopinath, and M. E. Siemens, "Quantitative measurement of the orbital angular momentum of light with a single, stationary lens," Opt. Lett. **41**(21), 5019–5022 (2016).
14. V. V. Kotlyar, A. A. Kovalev, and A. P. Porfirev, "Calculation of fractional orbital angular momentum of superpositions of optical vortices by intensity moments," Opt. Express **27**(8), 11236–11251 (2019).
15. V. V. Kotlyar, S. N. Khonina, and V. A. Soifer, "Light field decomposition in angular harmonics by means of diffractive optics," J. Mod. Opt. **45**(7), 1495–1506 (1998).
16. A. V. Volyar, M. V. Brezko, Y. E. Akimova, and Y. A. Egorov, "Beyond the intensity or intensity moments and measuring the spectrum of optical vortices in complex beams," CO **42**(5), 736–743 (2018).
17. A. V. Volyar, M. V. Brezko, Y. E. Akimova, Y. A. Egorov, and V. V. Milyukov, "Sector perturbation of a vortex beam: Shannon entropy, orbital angular momentum and topological charge," CO **43**(5), 723–734 (2019).
18. A. E. Siegman, Lasers (University Science, 1986).
19. F. Gori, G. Guattary, and C. Padovani, "Bessel-Gauss beams," Opt. Commun. **64**(6), 491–495 (1987).
20. M. S. Soskin, V. N. Gorshkov, M. V. Vastnetsov, J. T. Malos, and N. R. Heckenberg, "Topological charge and angular momentum of light beams carrying optical vortex," Phys. Rev. A **56**(5), 4064–4075 (1997).
21. A. A. Kovalev, V. V. Kotlyar, and A. P. Porfirev, "Asymmetric Laguerre-Gaussian beams," Phys. Rev. A **93**(6), 063858 (2016).
22. V. V. Kotlyar, A. A. Kovalev, R. V. Skidanov, and V. A. Soifer, "Asymmetric Bessel-Gauss beams," J. Opt. Soc. Am. A **31**(9), 1977–1983 (2014).
23. V. V. Kotlyar, A. A. Kovalev, and E. G. Abramochkin, "Kummer laser beams with a transverse complex shift," J. Opt. **22**(1), 015606 (2020).
24. V. V. Kotlyar and A. A. Kovalev, "Hermite-Gaussian modal laser beams with orbital angular momentum," J. Opt. Soc. Am. A **31**(2), 274–282 (2014).
25. V. V. Kotlyar, A. A. Kovalev, and A. P. Porfirev, "Vortex Hermite-Gaussian laser beams," Opt. Lett. **40**(5), 701–704 (2015).
26. A. Y. Bekshaev, M. S. Soskin, and M. V. Vasnetsov, "Optical vortex symmetry breakdown and decomposition of the orbital angular momentum of light beams," J. Opt. Soc. Am. A **20**(8), 1635–1643 (2003).
27. V. G. Volostnikov and E. G. Abramochkin, The modern optics of the Gaussian beams [In Russian] (Fizmatlit Publisher: Moscow, 2010).
28. V. V. Kotlyar, A. A. Kovalev, and A. V. Volyar, "Topological charge of a linear combination of optical vortices: topological competition," Opt. Express **28**(6), 8266–8281 (2020).
29. I. S. Gradshteyn and I. M. Ryzhik, Table of Integrals, Series, and Products (Academic: New York, 1965).